Universiteit
Leiden
The Netherlands

Global photometric structure of the Orion nebula

Greve, A.; Genderen, A.M. van; Augusteijn, T.

Citation

Greve, A., Genderen, A. M. van, & Augusteijn, T. (1993). Global photometric structure of the Orion nebula. *Astronomy And Astrophysics Supplement Series*, *99*, 577-584. Retrieved from https://hdl.handle.net/1887/7092

Version: Not Applicable (or Unknown)

License: Leiden University Non-exclusive license

Downloaded from: https://hdl.handle.net/1887/7092

Note: To cite this publication please use the final published version (if applicable).

1993A&AS...99..577G

ASTRONOMY & ASTROPHYSICS
SUPPLEMENT SERIES

Astron. Astrophys. Suppl. Ser. **99**, 577-584 (1993)

Global photometric structure of the Orion nebula*

A. Greve[1], A.M. van Genderen[2] and Th. Augusteijn[3]

[1] IRAM, Nucleo Central, Avda. Divina Pastora 7, 18102 Granada, Spain
[2] Sterrewacht Leiden, Postbus 9513, 2300 RA Leiden, The Netherlands
[3] Sterrenkundig Instituut "Anton Pannekoek", Kruislaan 403, 1098 SJ Amsterdam, The Netherlands

Received August 24; accepted September 28, 1992

Abstract. — We present Walraven *VBLUW* photometric observations of the Orion nebula. For an idealized radial-symmetric nebula the brightness distribution decreases exponentially with distance from the Trapezium stars. The integrated brightness and colour is calculated.

Key words: interstellar medium: HII regions: individual: Orion nebula — photometry

1. Introduction

The Orion nebula is a (the) prototype object for investigations of HII regions excited by OB stars. The large amount of observational data is compiled by Goudis (1982), however, only few (broad passband) photometric observations are reported. The lack of such data (for emission nebulae in general) is due to the fact that the astrophysical interpretation of photometric observations is not straightforward – if possible at all – (cf. Greve & van Genderen 1987, Paper I) because the observed fluxes contain a combination of line emission, atomic continuum radiation and scattered stellar light, usually of unknown ratio and changing with position in the nebula. Nevertheless, detailed photometric observations of emission nebulae may give information on the global structure and the integrated brightness distribution. To illustrate this case, we present Walraven *VBLUW* photometric observations of the Orion nebula. We are aware, however, that the *VBLUW* system (as any other photometric system designed for stellar observations) is not optimized for observations of emission nebulae.

2. Observations and reductions

The observations were made in 1986 with the Walraven *VBLUW* photometer (Walraven & Walraven 1960; Rijf et al. 1969; Lub & Pel 1977) attached to the 90 cm Dutch telescope, ESO, La Silla. The data refer to the upgraded photometric system in use since 1980, as given in Table 1, and the corresponding absolute calibration published by de Ruyter & Lub (1986). Unfortunately, the photometric system has been taken out of operation in 1991.

Table 1. Parameters of the Walraven *VBLUW* photometric system

Passband	V	B	L	U	W
Effect. wavel. (A)*	5441	4298	3837	3623	3235
Bandwidth (FHW,A)*	708	423	221	232	157

* A = Angstrom

We comment on scattered light in the atmosphere and in the telescope for nebular measurements made close to bright stars (cf. Paper I). Using a 23″ diameter diaphragm, at 30″ distance from a bright star (magnitude ≈ 6) the measured amount of scattered light was $\leq 1/1000$ of the stellar flux, for all passbands. Reduced to a diaphragm of $1('')^2$ area, this amount of scattered light is ≥ 13.2 mag$/('')^2$ fainter than the star. Thus, for distances greater than approximately 30″ the nebular emission dominates the instrumentally scattered light of the Trapezium stars.

Table 2 gives the positions of the observations as offsets in RA and Dec. from the Trapezium star Θ^1 ORI C; these positions are shown in Fig. 1. The measurements are confined to the central region of the nebula of $\sim 400''$ radius and are not made with homogeneous spatial coverage. As listed in Table 2, some of the observations were made at positions for which spectroscopic data are available (indicated in Table 2 by the notation of Kaler 1976,

* Based on data collected at ESO, La Silla, Chile

© European Southern Observatory • Provided by the NASA Astrophysics Data System

1993A&AS...99..577G

and listed below in the references). Additional $VBLUW$ observations of the Orion nebula were reported earlier in Paper I; these data are included in Table 2.

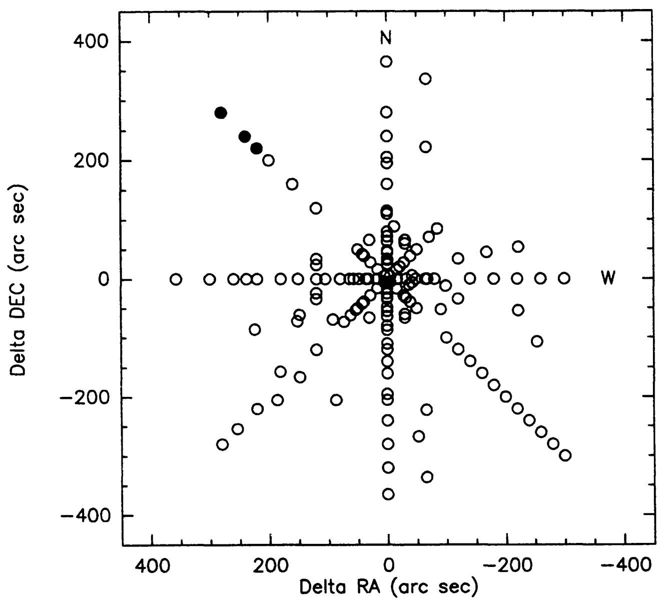

Fig. 1. Positions of the photometric measurements; the center position coincides with the star Θ^1 ORI C. The solid dots refer to measurements in the dark bay area of the nebula

The photometric measurements are also given in Table 2; in the $VBLUW$ system the data are logarithms of intensity. A 16″ diameter diaphragm was used. The observations are corrected for sky background; the data are *not* corrected for (foreground) reddening which is of the order of $A_V \approx 1$ mag. (cf. Chaisson & Dopita 1977; Goudis 1982). The de-reddening relations of the $VBLUW$ system are given by Lub & Pel (1977).

The apparent visual magnitude V_J and the colour index $(B-V)_J$ of the Johnson UBV system (denoted by the index J), as given in Table 2, are calculated from the relations (Pel 1986)

$$V_J = 6.886 - 2.5[V + 0.033(V - B)] \quad (1)$$

and

$$(B-V)_J = 2.571(V-B) - 1.020(V-B)^2 + 0.500(V-B)^3 - 0.010 \quad (2)$$

The data of the UBV system are given in magnitudes. The relations (1) and (2) are derived for stars (i.e. continuum sources), however, for emission nebulae these transformations are expected to give values V_J and $(B-V)_J$ which are correct within $\leq |0.1|$ mag.

We assume a homogeneous brightness inside the area $(= 201('')^2)$ of the 16″ diaphragm, and we assume radial symmetry of the spatial brightness distribution with Θ^1 ORI C as center. This is a highly idealized picture, in particular when compared with the current blister model of the Orion nebula (cf. Rubin et al. 1991; Baldwin et al. 1991). However, the relatively small scatter of the brightness distribution with respect to a *linear* radial dependence, as shown in the figures below, indicates that this assumption is a physically useful hypothesis, as also used by other observers (cf. Simpson 1973).

3. Global photometric structure

Figure 2 shows the brightness V_J, per 1 $('')^2$ area, *not* corrected for reddening, as function of the radial distance r from the Trapezium star Θ^1 ORI C. There exists a scatter in the brightness of ≈ 1 mag/$('')^2$, however, when assuming radial symmetry of the nebula the large–scale, global brightness distribution for the region $\sim 30 \leq r \leq 400''$ can be approximated by the linear relation

$$V_J(r) = a_V + b_V r = 15.39 + 0.011r \quad (3)$$

with r in arcseconds (″) and $V_J(r)$ in mag/$('')^2$. The coefficients a_V, b_V were determined by a least squares fit and the corresponding linear approximation is shown in Fig. 2. The V passband ($\approx V_J$) contains mainly continuum radiation and (many) weak lines with strengths of a few percent of H_β (cf. Johnson 1968; Osterbrock et al. 1992). However, the strength of the atomic continuum is related to the strength of H_β so that a correlation of V_J and the intensity of H_β is expected to exist in case scattered stellar light does not dominate the flux (for scattered stellar light see O'Dell & Hubbard 1965, Münch & Persson 1971, Simpson 1973, Schiffer & Mathis 1974, Perrin & Sivan 1992). Such a correlation is shown in Fig. 2 with the intensity of H_β taken from Dopita et al. (1975) and here expressed in magnitudes.

Denoting by $I_{VJ}(r)$ the intensity measured in the V_J passband, per 1 $('')^2$ area, Eq. (3) represents an exponential spatial distribution of the intensity

$$I_{VJ}(r) = I_{VJ}(0)\ \exp(-0.011r) = 6.98\ 10^{-7}\ \exp(-0.011r) \quad (4)$$

The intensity $I_{VJ}(R)$ emitted from the circular area inside the radius R is

$$I_{VJ}(R) = 2\pi\ I_{VJ}(0) \int_0^R r\ \exp(-0.011r)\mathrm{d}r \quad (5)$$

Table 3 gives the values $I_{VJ}(R)$ in magnitudes, there denoted $V_J(R)$. Similarly, from Eq. (1) and Eq. (2) we obtain for the B_J passband

$$I_{BJ}(r) = I_{BJ}(0)\ \exp(-0.0084r) = 4.02\ 10^{-7}\ \exp(-0.0084r) \quad (6)$$

Table 3 gives also the integrated values $I_{BJ}(R)$ in magnitudes, there denoted $B_J(R)$, and the colours $(B-V)_J(R)$. We extrapolated the observations to $r =$

© European Southern Observatory • Provided by the NASA Astrophysics Data System

1993A&AS...99..577G

Table 3. Brightness and colours (Johnson UBV system) of the Orion nebula assuming radial symmetry

r(")	100	200	300	400	600+	800+	infinit
VJ(r)	16.5	17.6	18.1	19.8	22.0	24.2	
BJ(r)	16.9	17.8	18.7	19.6	21.4	23.3	
(B-V)J(r)	0.48	0.21	0.01	-0.19	-0.58	-0.98	
VJ(R)++	4.85	3.98	3.67	3.53	3.45	3.44	3.44
BJ(R)	5.33	4.36	3.97	3.79	3.65	3.62	3.61
(B-V)J(R)	0.48	0.38	0.30	0.26	0.20	0.18	0.17
PV(R) (%)	27	61	81	92	99		
PB(R) (%)	20	50	72	85	96	99	

\+ extrapolated from Eq.(4); the measurements are confined to ~ 400"
VJ(r), BJ(r) in mag/(")**2
(B-V)J(r), VJ(R), BJ(R), (B-V)J(R) in magnitudes
++ VJ = 4.69 for the combination of the Theta 1 ORI stars A+B+C+D.

600″, 800″, and 'infinity', and calculated the corresponding integrated brightness and colour as given in Table 3. This table gives also the relative amount of energy emitted in different circular sections, denoted $P_V(R) = I_{VJ}(R)/I_{VJ}(\infty)$ and $P_B(R) = I_{BJ}(R)/I_{BJ}(\infty)$, respectively.

From relation (4) and (6), respectively, we derive that the emission of the nebula falls to 1/2 of the emission at its center at a radial distance of ~ 0.15 pc for V_J and ~ 0.20 pc for B_J, when adopting a distance of the Orion nebula of 500 pc.

Figure 3 shows that for the other passbands of the Walraven system the logarithms of the measured intensities B, L, U, W follow also a linear radial dependence. The corresponding coefficients a_B, b_B, a_L, b_L etc. of the relations

$$B = a_B + b_B r, \qquad L = a_L + b_L r, \quad .... \tag{7}$$

etc. are given in Table 4; the corresponding linear relations are shown in Fig. 3.

Table 4. Coefficients a, b of Eq. (7)

Passband (eff. wavel., A)	a	b
V(5441)	-3.328	-0.00476
B(4298)	-3.545	-0.00393
L(3897)	-3.416	-0.00386
U(3623)	-3.423	-0.00382
W(3235)	-3.693	-0.00384

Units: [a] = log. int./(")**2
[b] = log. int./(")**2/(")

In Fig. 3 there are three positions (between $280'' \leq r \leq 400''$) where the intensities are significantly lower than those measured at similar radial distances and as derived from the linear approximations. The positions of these observations are especially marked in Figure 1; they are located in the dark bay area at the NE of the nebula at d(RA) and d(Dec) = (280″, 280″), (240″, 240″), and (200″, 200″). When we use relation (3) to characterize the "average" nebula we find from the observations that at these positions of the dark bay there exists an additional (foreground) extinction of $A_V \approx 1$ mag, which is in agreement with the values obtained by Chaisson & Dopita (1977).

4. Walraven colours

While the intensities (logarithms) of the $VBLUW$ passbands show a convincing linear radial dependence, the conventional colours of the Walraven system do not exhibit such a feature. Figure 4 shows the measured colours as function of radial distance from the Trapezium stars. In these diagrams the colours change from below to the top from red to blue. For all colours there are significant offsets from the stellar colours; for $(B - L)$ and $(B - U)$ the nebular colours are systematically more blue than the stellar colour, for $(U - W)$ they are systematically more red than the stellar colour, and these offsets remain nearly constant (though with a large scatter) throughout the nebula. For $(V - B)$ the nebula is more red in the vicinity of the Trapezium stars, and gradually the colour changes to more blue in the outer regions. This may be an effect of a changing contribution of scattered stellar light.

The solid and dashed lines in Fig. 4 show the colour dependence for cuts across the nebula in the direction NS and EW. These cuts reveal no particular features of the colour distribution.

5. Conclusion

For radiation in the wavelength region from ~ 3200 Å to ~ 5500 Å, as measured through the filters of the Walraven photometric system, the Orion nebula shows an exponential radial decrease of the emission and considerable radial symmetry with the Trapezium stars as center. The photometric 'half-width' of the nebula is $0.15 - 0.20$ pc.

Acknowledgements. We thank the staff of ESO, La Silla (Chile), for their help in the observations and the logistics support.

References

Baldwin J.A., Ferland G.J., Martin P.G., Corbin M.R., Cota S.A., Peterson B.M., Slettebak A. 1991, ApJ 374, 580
Bohuski T.J., Dufour R.J., Osterbrock D.E. 1974, ApJ 188, 529 (BDO)
Boyce P.B. 1966, Lowell Obs. Bull. 6, 215 (BO)
Chaisson E.J., Dopita M.A. 1977, A&A 56, 385
de Ruyter H.R., Lub J. 1986, A&AS 63, 59
Dopita M.A., Isobe S., Meaburn J. 1975, Ap&SS 34, 91
Goudis C. 1982, The Orion Complex, D. Reidel Publ. Co., Dordrecht

© European Southern Observatory • Provided by the NASA Astrophysics Data System

1993A&AS...99..577G

Greve A., van Genderen A.M. 1987, A&A 174, 243 (Paper I)

Johnson H.M. 1968, Diffuse Nebulae, in Nebulae and Interstellar Matter, Stars and Stellar Systems, Vol. II, ed. B.M. Middlehurst, L.H. Aller, Univ. Chicago Press, p. 65

Kaler J.B. 1976, ApJS 31, 517

Kaler J.B., Lien D., Peck M. 1979, ApJ 234, 909 (KLP)

Lub J., Pel J.W. 1977, A&A 54, 137

Mendez M.E. 1967, Boll. Obs. Ton. 4, 91 (ME67)

Mendez M.E. 1968, Boll. Obs. Ton. y Tac. 4, 240 (ME68)

Münch G., Persson S.E. 1971, ApJ 165, 241

O'Dell C.R., Hubbard W.B. 1965, ApJ 142, 591

Osterbrock D.E., Tran H.D., Veilleux S. 1992, ApJ 389, 305

Peimbert M., Torres-Peimbert S. 1977, MN 179, 217 (PTP4)

Pel W. 1986, Intern. Report, Leiden

Perrin J.M., Sivan J.P. 1992, A&A 255, 271

Razmadze N.A. 1958, Bull. Abastumani AP. Obs. No. 23, p. 91 (also Astr. Zh. 156, 33, 698) (R1)

Rijf R., Tinbergen J., Walraven Th. 1969, Bull. Astron. Inst. Netherlands 20, 279

Rubin R.H., Simpson J.P., Haas M.R., Erickson E.F. 1991, ApJ 374, 564

Schiffer F.H., Mathis J.S. 1974, ApJ 194, 597

Simpson J.P. 1973, PASP 85, 479

Tamura S. 1976, Sci. Rep. Tohoku Univ. 59, 1 (TAM2)

Torres-Peimbert S., Peimbert M. 1980, ApJ 238, 133 (TPD)

Walraven Th., Walraven J. 1960, Bull. Astron. Inst. Netherlands 15, 67

© European Southern Observatory • Provided by the NASA Astrophysics Data System

1993A&AS...99..577G

Table 2. *VBLUW* colours of the Orion nebula (16″ diaphragm)

dRA*	dDec*	V	(V-B)	(B-U)	(U-W)	(B-L)	VJ	(B-V)J	Ref.
		(		log. intensity		)	(	mag.)	**
Averaged Trapezium stars (Theta 1 ORI A+B+C+D)									
0	0	0.920	0.028	-0.039	-0.141	-0.008	4.6	-0.05	
EMISSION NEBULA									
Direction N - S									
0	-365	-2.807	-0.069	-0.271	0.056	-0.179	13.9	-0.19	BDO-8
0	-320	-2.555	-0.005	-0.240	0.158	-0.171	13.3	-0.02	
0	-280	-2.364	-0.014	-0.245	0.117	-0.160	12.8	-0.05	BDO-7
0	-240	-2.310	-0.002	-0.270	0.189	-0.190	12.7	-0.02	
0	-205	-2.284	0.015	-0.259	0.164	-0.174	12.6	0.03	KLP-2
0	-195	-2.234	0.016	-0.272	0.177	-0.190	12.5	0.03	BDO-6
0	-160	-1.996	0.035	-0.280	0.188	-0.189	11.9	0.08	
0	-140	-1.579	0.079	-0.355	0.295	-0.255	10.8	0.19	TPD-3
0	-120	-1.335	0.168	-0.364	0.289	-0.263	10.2	0.39	R1-2
0	-110	-1.363	0.200	-0.300	0.243	-0.222	10.3	0.46	BDO-5
0	-87	-1.410	0.197	-0.243	0.184	-0.167	10.4	0.46	ME67-7
0	-80	-1.344	0.240	-0.248	0.188	-0.173	10.2	0.55	
0	-64	-1.270	0.254	-0.246	0.192	-0.175	10.0	0.58	
0	-55	-1.313	0.218	-0.267	0.226	-0.198	10.2	0.50	ME67-10
0	-48	-1.226	0.258	-0.269	0.226	-0.200	9.93	0.59	
0	-34	-1.185	0.308	-0.233	0.211	-0.173	9.8	0.69	KLP-1, PTP-4
0	-32	-1.165	0.326	-0.252	0.229	-0.187	9.8	0.72	
0	-25	-1.127	0.310	-0.215	0.187	-0.163	9.7	0.69	BDO-4
0	-16	-1.504	0.318	-0.214	0.162	-0.160	10.6	0.71	
0	25	-1.115	0.235	-0.151	0.173	-0.117	9.7	0.54	
0	32	-1.186	0.284	-0.220	0.166	-0.163	9.8	0.64	
0	34	-1.212	0.264	-0.221	0.172	-0.163	9.9	0.60	BDO-1, PTP4-3A
0	45	-1.181	0.282	-0.249	0.201	-0.180	9.8	0.64	PTPD4-1A, TPD-7
0	48	-1.185	0.310	-0.269	0.223	-0.200	9.8	0.69	
0	64	-1.333	0.265	-0.271	0.232	-0.201	10.2	0.60	
0	72	-1.421	0.231	-0.255	0.223	-0.184	10.4	0.53	ME68-P
0	80	-1.395	0.265	-0.276	0.240	-0.201	10.3	0.60	
0	110	-1.569	0.166	-0.280	0.226	-0.194	10.8	0.39	
0	115	-1.592	0.162	-0.292	0.245	-0.204	10.9	0.38	ME67-9, BDO-2
0	160	-1.808	0.086	-0.331	0.282	-0.244	11.4	0.20	
0	195	-1.972	0.060	-0.262	0.202	-0.185	11.8	0.14	
0	205	-2.060	0.069	-0.234	0.201	-0.176	12.0	0.16	BDO-3
0	240	-2.235	0.081	-0.195	0.179	-0.136	12.5	0.19	
0	280	-2.381	0.085	-0.168	0.135	-0.114	12.8	0.20	
0	280	-2.394	0.080	-0.169	0.141	-0.121	12.9	0.19	
0	365	-2.276	0.047	-0.140	0.153	-0.092	12.6	0.11	KLP-3
Direction W-E									
-300	0	-2.465	0.044	-0.342	0.226	-0.242	13.0	0.10	
-260	0	-2.404	0.051	-0.312	0.202	-0.220	12.9	0.12	
-220	0	-2.233	0.083	-0.328	0.215	-0.224	12.5	0.20	
-180	0	-2.110	0.108	-0.312	0.201	-0.222	12.2	0.26	
-140	0	-1.874	0.141	-0.315	0.214	-0.232	11.6	0.33	
-80	0	-1.406	0.220	-0.273	0.205	-0.196	10.4	0.51	
-68	0	-1.286	0.210	-0.295	0.232	-0.217	10.1	0.49	ME67-2
-64	0	-1.215	0.262	-0.292	0.236	-0.217	9.9	0.59	
-48	0	-1.035	0.280	-0.302	0.262	-0.228	9.4	0.63	
-32	0	-0.887	0.326	-0.266	0.233	-0.197	9.1	0.72	
-16	0	-0.869	0.280	-0.192	0.159	-0.137	9.0	0.63	
16	0	-0.170	0.000	-0.077	-0.058	-0.011	7.3	0.01	
32	0	-1.281	0.321	-0.214	0.156	-0.154	10.1	0.71	
32	0	-1.304	0.280	-0.211	0.160	-0.154	10.1	0.63	ME67-3
36	0	-1.329	0.277	-0.225	0.173	-0.161	10.2	0.62	ME68-E
48	0	-1.492	0.231	-0.266	0.190	-0.194	10.6	0.53	
57	0	-1.624	0.167	-0.249	0.167	-0.176	10.9	0.39	ME68-F
64	0	-1.574	0.200	-0.239	0.155	-0.174	10.8	0.46	
80	0	-1.511	0.192	-0.256	0.176	-0.186	10.6	0.45	
105	0	-1.845	0.060	-0.201	0.101	-0.141	11.5	0.14	ME67-6, ME68-A
120	0	-1.903	0.045	-0.184	0.084	-0.127	11.6	0.10	BDO-11
151	0	-1.885	0.042	-0.202	0.133	-0.139	11.6	0.10	ME67-5
180	0	-2.066	0.032	-0.199	0.133	-0.143	12.1	0.07	
220	0	-2.068	0.030	-0.203	0.156	-0.140	12.1	0.07	
238	0	-2.091	0.031	-0.164	0.116	-0.112	12.1	0.07	BDO-12
260	0	-2.249	0.029	-0.157	0.118	-0.108	12.5	0.06	
300	0	-2.440	0.050	-0.151	0.127	-0.108	12.9	0.12	
357	0	-2.464	0.059	-0.180	0.192	-0.132	13.0	0.14	BDO-13

© European Southern Observatory • Provided by the NASA Astrophysics Data System

1993A&AS...99..577G

Table 2. continued

Direction NE - SW

280	280	-2.991	0.124	-0.088	0.142	-0.040	14.4	0.29	
240	240	-3.005	0.122	-0.107	0.155	-0.080	14.4	0.29	
200	200	-2.956	0.104	-0.166	0.177	-0.116	14.3	0.25	
160	160	-2.351	0.094	-0.139	0.123	-0.099	12.8	0.22	
120	120	-1.876	0.097	-0.280	0.276	-0.206	11.6	0.23	
50	50	-1.847	0.186	-0.212	0.200	-0.146	11.5	0.43	
42	42	-1.269	0.232	-0.269	0.185	-0.193	10.0	0.53	R1-9
39	39	-1.777	0.184	-0.254	0.209	-0.176	11.3	0.43	
28	28	-1.740	0.194	-0.219	0.153	-0.148	11.2	0.45	
16	16	-1.410	0.216	-0.215	0.135	-0.156	10.4	0.50	
5	5	-0.130	0.123	0.054	0.115	-0.008	7.2	0.29	
-5	-5	-0.954	0.308	-0.241	0.201	-0.176	9.2	0.69	
-16	-16	-1.131	0.253	-0.266	0.223	-0.187	9.7	0.58	
-28	-28	-1.453	0.226	-0.285	0.209	-0.208	10.5	0.52	
-32	-32	-1.104	0.205	-0.267	0.237	-0.191	9.6	0.47	ME67-1
-39	-39	-1.619	0.193	-0.269	0.176	-0.190	10.9	0.45	
-50	-50	-1.821	0.204	-0.255	0.166	-0.170	11.4	0.47	
-100	-100	-1.723	0.195	-0.296	0.202	-0.203	11.2	0.45	
-120	-120	-1.910	0.160	-0.316	0.216	-0.221	11.6	0.38	
-140	-140	-1.994	0.137	-0.347	0.242	-0.248	11.9	0.32	
-160	-160	-2.186	0.080	-0.337	0.217	-0.240	12.3	0.19	
-180	-180	-2.307	0.052	-0.330	0.206	-0.240	12.7	0.12	
-200	-200	-2.378	0.026	-0.318	0.200	-0.237	12.8	0.06	
-220	-220	-2.433	0.014	-0.408	0.296	-0.306	13.0	0.03	
-240	-240	-2.515	0.002	-0.390	0.270	-0.286	13.2	0.00	
-260	-260	-2.583	-0.001	-0.384	0.271	-0.282	13.3	-0.01	
-280	-280	-2.635	-0.019	-0.393	0.310	-0.295	13.5	-0.06	
-300	-300	-2.706	-0.018	-0.380	0.294	-0.293	13.7	-0.06	

Direction SE - NW

280	-280	-2.593	-0.082	-0.422	0.339	-0.308	13.4	-0.23	
220	-220	-2.261	-0.048	-0.349	0.250	-0.248	12.5	-0.14	
120	-120	-1.789	-0.030	-0.288	0.167	-0.199	11.4	-0.09	
73	-73	-1.251	0.164	-0.324	0.252	-0.227	10.0	0.38	ME67-4
62	-62	-1.313	0.205	-0.285	0.211	-0.198	10.2	0.47	ME68-G, TAM2-5
53	-53	-1.309	0.212	-0.282	0.202	-0.199	10.1	0.49	ME68-H
50	-50	-1.131	0.032	-0.251	0.164	-0.166	10.2	0.07	
42	-42	-1.278	0.230	-0.265	0.179	-0.191	10.1	0.53	R1-1
39	-39	-1.197	0.234	-0.302	0.230	-0.209	9.9	0.54	
28	-28	-1.254	0.254	-0.276	0.196	-0.198	10.0	0.58	
16	-16	-1.187	0.292	-0.258	0.174	-0.191	9.8	0.66	
5	-5	-1.266	0.294	-0.211	0.148	-0.162	10.0	0.66	
-5	5	-0.713	0.276	-0.098	0.153	-0.062	8.6	0.62	
-16	16	-1.069	0.320	-0.257	0:212	-0.186	9.5	0.71	
-21	21	-0.997	0.258	-0.260	0.229	-0.189	9.4	0.59	
-28	28	-1.154	0.282	-0.321	0.274	-0.238	9.7	0.64	
-39	39	-1.420	0.208	-0.352	0.295	-0.265	10.4	0.48	
-50	50	-1.552	0.195	-0.350	0.278	-0.261	10.7	0.45	
-71	71	-1.448	0.170	-0.332	0.281	-0.245	10.5	0.40	ME67-8
-85	85	-1.588	0.166	-0.347	0.286	-0.253	10.8	0.39	R1-2

Other positions

-254	-107	-2.331	0.057	-0.298	0.191	-0.214	12.7	0.13	TAM2-15
-222	-54	-2.267	0.088	-0.285	0.159	-0.193	12.5	0.21	BO-D
-222	54	-2.288	0.059	-0.363	0.241	-0.255	12.6	0.14	
-168	45	-2.078	0.079	-0.328	0.208	-0.238	12.1	0.19	PTP4-1B
-120	34	-1.861	0.100	-0.342	0.242	-0.254	11.5	0.24	
-120	-34	-1.868	0.119	-0.301	0.168	-0.214	11.5	0.28	BDO-9
-99	-12	-1.716	0.174	-0.262	0.165	-0.188	11.2	0.41	TAM2-12
-91	-52	-1.612	0.176	-0.321	0.229	-0.236	10.9	0.41	TAM2-10
-66	-336	-2.630	-0.026	-0.262	0.163	-0.188	13.5	-0.08	BO-H
-66	-222	-2.282	-0.005	-0.267	0.149	-0.186	12.6	-0.02	BO-G
-66	336	-2.478	0.083	-0.165	0.170	-0.124	13.1	0.20	
-66	222	-2.057	0.031	-0.344	0.285	-0.258	12.0	0.07	
-52	-267	-2.486	0.025	-0.221	0.152	-0.167	13.1	0.05	TAM2-13
-42	-6	-0.986	0.242	-0.305	0.265	-0.228	9.3	0.55	
-42	6	-0.955	0.286	-0.274	0.238	-0.200	9.2	0.64	BO-A
-37	-10	-0.946	0.248	-0.297	0.256	-0.221	9.2	0.57	TPD-2
-30	-66	-1.299	0.218	-0.273	0.201	-0.199	10.1	0.50	BO-E
-30	-60	-1.301	0.221	-0.273	0.208	-0.201	10.1	0.51	
-30	66	-1.422	0.238	-0.296	0.264	-0.220	10.4	0.54	
-30	60	-1.317	0.233	-0.312	0.268	-0.231	10.2	0.53	BO-C
-12	89	-1.451	0.216	-0.290	0.257	-0.211	10.5	0.50	TAM2-11
30	-66	-1.223	0.210	-0.261	0.180	-0.185	9.9	0.49	BO-F
30	66	-1.443	0.216	-0.250	0.191	-0.183	10.5	0.50	
87	-205	-2.050	-0.033	-0.352	0.250	-0.251	12.0	-0.10	TPD-7B
92	-69	-1.252	0.094	-0.385	0.315	-0.280	10.0	0.22	TAM2-6
120	-34	-1.338	0.113	-0.357	0.256	-0.256	10.2	0.27	BDO-10
120	-24	-1.384	0.135	-0.319	0.226	-0.230	10.3	0.32	BO-B
120	34	-2.388	0.106	-0.184	0.143	-0.128	12.8	0.25	
120	24	-2.293	0.098	-0.180	0.138	-0.121	12.6	0.23	
148	-166	-1.977	-0.048	-0.338	0.223	-0.239	11.8	-0.14	TPD-6C
148	-61	-1.697	-0.040	-0.292	0.189	-0.201	11.1	-0.11	TPD-3C
152	-72	-1.712	-0.044	-0.287	0.178	-0.194	11.2	-0.13	TAM2-7
181	-157	-2.064	-0.050	-0.325	0.215	-0.229	12.1	-0.14	TAM2-9
186	-205	-2.167	-0.061	-0.340	0.244	-0.236	12.3	-0.17	TPD-7A
224	-86	-1.971	-0.007	-0.284	0.208	-0.201	11.8	-0.03	TAM2-8
254	-254	-2.378	-0.057	-0.359	0.260	-0.254	12.8	-0.16	R1-7

* dRA = delta(RA) distance in RA from Theta 1 ORI C, in arcseconds.
* dDec = delta(Dec) distance in Dec from Theta 1 ORI C, in arcseconds.
** references of slit spectra taken at the same position; abbreviation: observers, after the dash: indication of the corresponding spectrum as used by the observers.

© European Southern Observatory • Provided by the NASA Astrophysics Data System

1993A&AS...99..577G

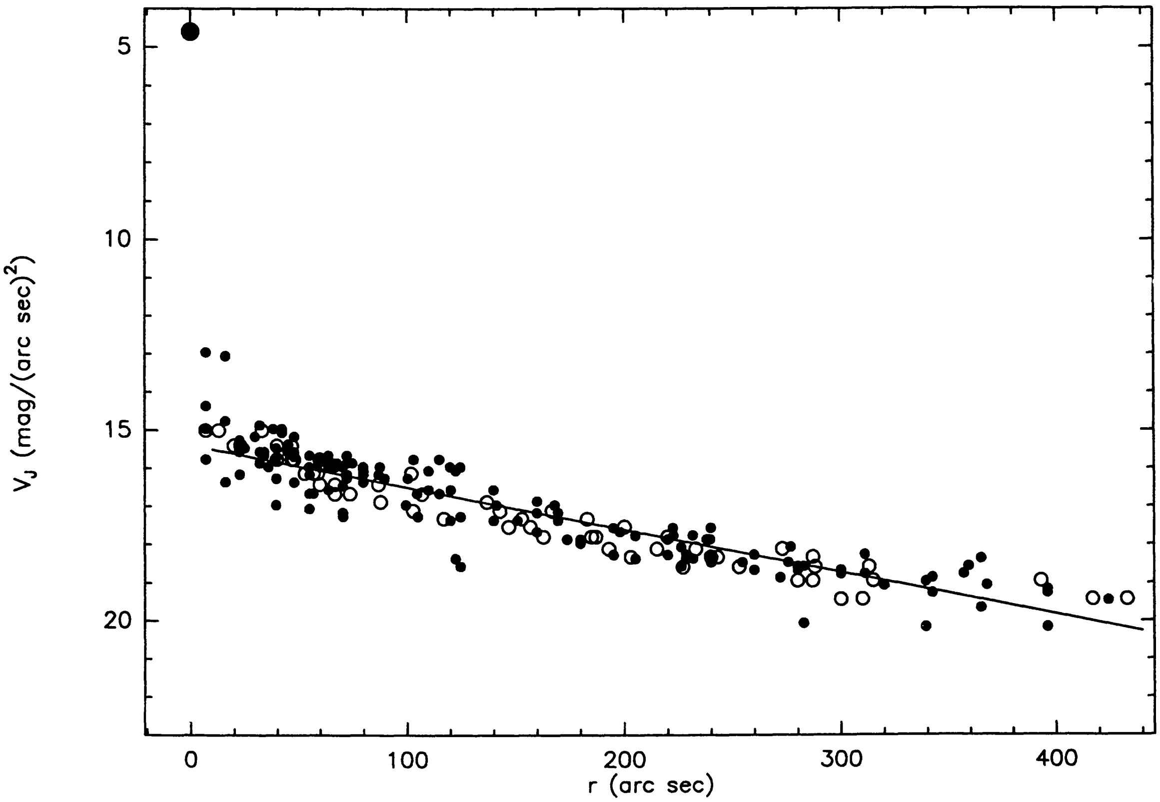

Fig. 2. Radial dependence of the visual magnitude V_J : small solid dots, with the linear fit inserted as calculated from Eq. (3). The open circles show the intensity of H_β (in magnitudes, adjusted scale) taken from Dopita et al. (1975). The large dot (at $r = 0$) gives the integrated brightness of the stars Θ^1 ORI A+B+C+D

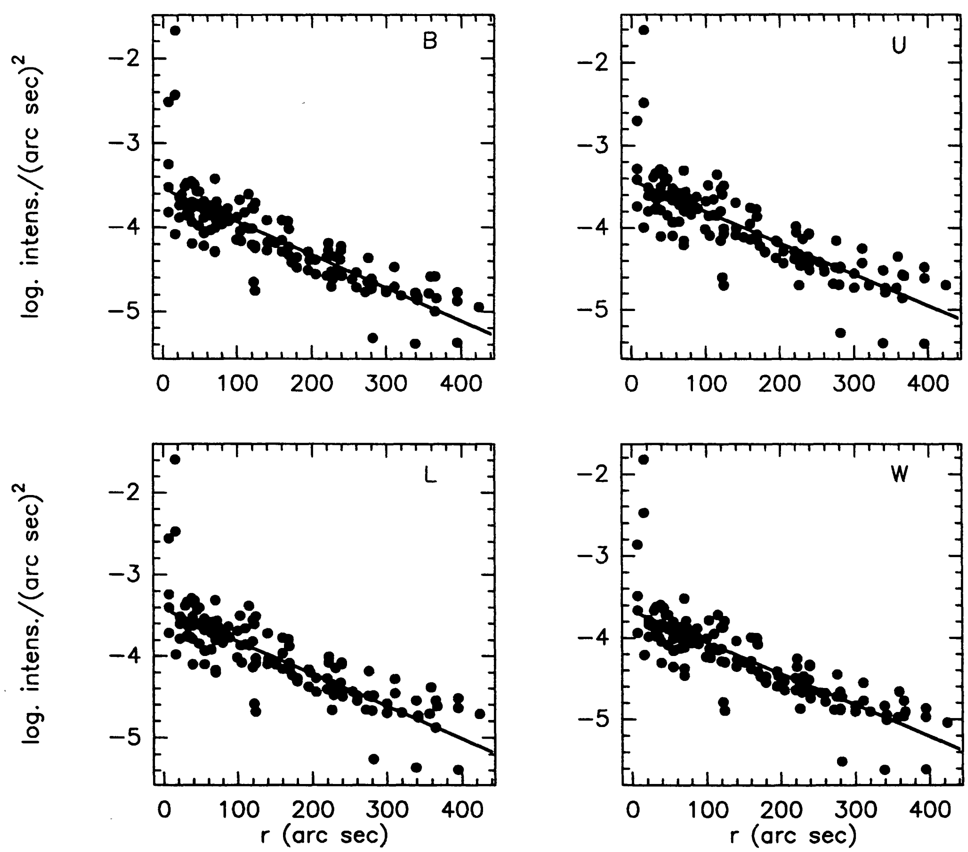

Fig. 3. Intensities (logarithms) measured in the passbands B, L, U, W and least squares fit linear relations (see Eq. (7)). The three measurements at $200'' \leq r \leq 400''$, which deviate from measurements at similar radial distances, are taken in the dark bay area of the nebula (see also Fig. 1)

© European Southern Observatory • Provided by the NASA Astrophysics Data System

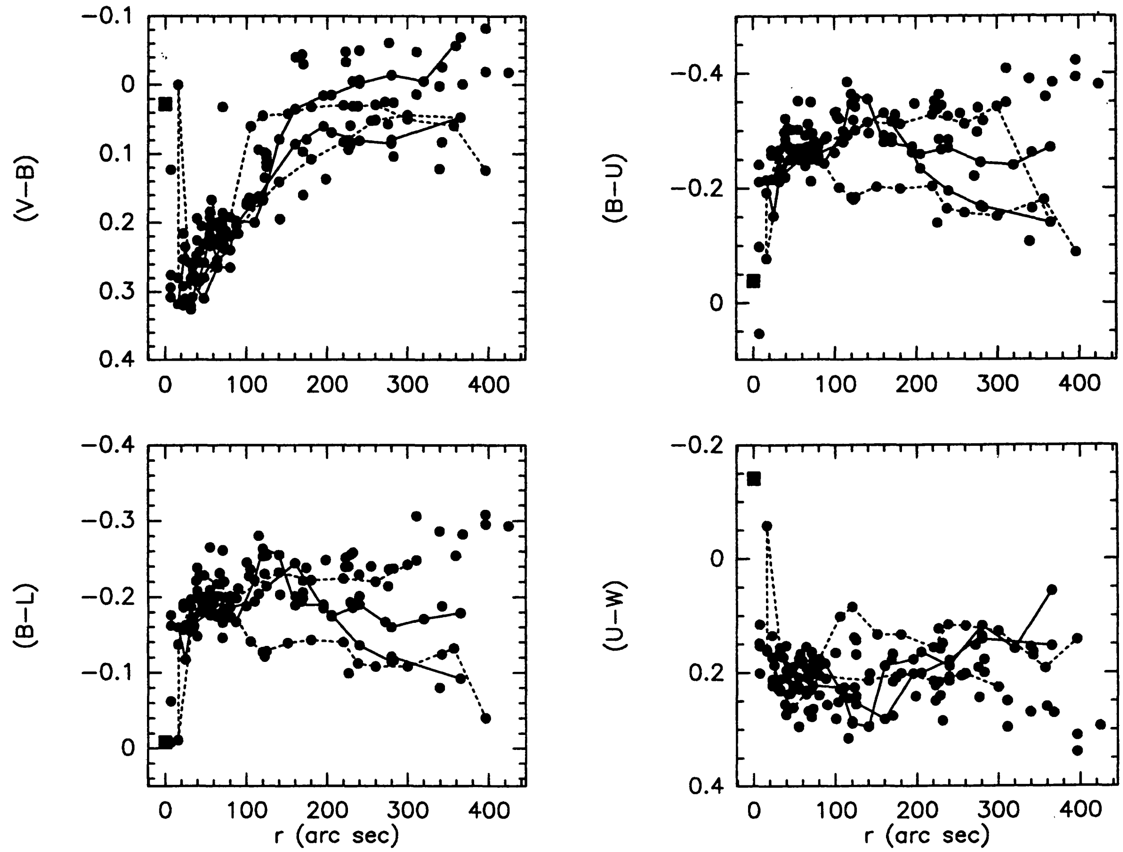

Fig. 4. Colours (solid dots) or the *VBLUW* system as function of radial distance from the star Θ^1 ORI C. The solide square is the integrated colour of the Trapezium stars Θ^1 ORI A+B+C+D. The solid lines and the dashed lines indicate cuts through the nebula in the directions NS and EW, respectively

1993A&AS...99..577G

© European Southern Observatory • Provided by the NASA Astrophysics Data System